Heat Transfer at the Phase-Interface of Condensing Bubbles

F. MAYINGER
Lehrstuhl A für Thermodynamik
Technische Universtät München, West-Germany
Arcisstrasse 21, D-8000 München 2, Germany

Y. M. CHEN
National Taiwan University, Taipei, Taiwan

D. NORDMANN
Lehrstuhl A für Thermodynamik
Technische Universtät München, West-Germany
Arcisstrasse 21, D-8000 München 2, Germany

Abstract

Condensing of a vapour bubble entering a subcooled liquid may be controlled by the heat transfer process at the phase interface or by inertia forces in the surrounding liquid. The limit for heat transfer controlled condensation can be expressed by the Jacob-number.
Heat transfer phenomena at the phase interface of vapour bubbles injected into subcooled water were investigated by using the holographic interferometry and the highspeed cinematography. Various substances like Ethanol, Propanol, refrigerant R113 and water were used and the phase interface process could be well described by correlations based on dimensionless numbers.

1. Introduction

The temporal course of the collapse of a vapour bubble during condensation in a subcooled liquid can be controlled by two different phenomena:

- The heat transfer at the phase interface of vapour and liquid and
- The inertia of the liquid mass when entering into the space set free by the condensing vapour.

The heat transfer process at the phase interface is influenced by the thermo-physical properties like heat conductivity, specific heat, latent heat of evaporation, density, viscosity and surface tension. Also the gradient of the saturation line plays a role. The thermo-physical properties can be expressed in dimensionless numbers like the Prandtl-number

$$Pr = \frac{\eta_F \, c_P}{\lambda_F} \tag{1}$$

and the Jacob-number

$$Ja = \frac{\varrho_F \, c_P \, (T_S - T_\infty)}{\varrho_D \, \Delta h_{FD}} \tag{2}$$

With bubbles moving in the liquid also the Reynolds-number

$$Re = \frac{2 R w \, \varrho_F}{\eta_F} \tag{3}$$

has to be taken into account with the relative velocity w_{rel} between the bubble and the liquid and the radius of the bubble as characteristic length. Finally the Fourier-number

$$Fo = \frac{a_F \, t}{(2R)^2} \tag{4}$$

can be used as a dimensionless time for describing the duration of the collapsing period.

There is a large number of theoretical and experimental studies in the literature dealing with condensation of bubbles. An extensive and comprehensive discussion of the status of art can be found for example in /1,2/. In the case of inertia controlled condensation Plesset /3/ and Hammit /4/ found good agreement with Rayleigh's correlation /5/. The situation with heat transport controlled condensation seems to be more complicated. Various authors describe the heat transfer at the phase interface of a condensing bubble similar to that around a moving solid sphere /6,7/ or a liquid droplet /8/. Examples of equations describing the bubble collaps are presented in Tab.1.

Author	Equation	Remarks
Florschuetz and Chao /9/	$\beta = \frac{R}{R_0} = 1 - \sqrt{\tau_H}$	$\tau_H = \frac{16}{\pi} \cdot Ja^2 \cdot Fo$
Voloshko and Vurgaft /10/	$\beta = 1 - 6{,}776 \cdot 10^{-4} \cdot Fo$	experimental $40 < Ja < 75$
Voloshko, Vurgaft and Aksel rod /8/	$\beta = \left[1 - \frac{5 \cdot K}{\sqrt{2} \cdot \pi} \cdot Ja \cdot Pe^{1/2} \cdot Fo\right]^{2/5}$	with $K = 1{,}88$ from experiment
Moalem and Sideman /6/	$\beta = \left[1 - \frac{3}{\sqrt{\pi}} \cdot Ja \cdot Pe^{1/2} \cdot Fo\right]^{5/7}$ $\beta = \left[1 - \frac{5}{2} \cdot \frac{1}{\sqrt{\pi}} \cdot Ja \cdot Pe^{1/2} \cdot Fo\right]^{2/5}$	for $2 < R_0 < 4mm$ for $R_0 < 1mm$
Akiyama /7/	$\beta = \left[1 - 2{,}8 \cdot C \cdot Pr^{-4/7} \cdot Ja \cdot Pe^{0{,}5} \cdot Fo\right]^{2/7}$	with $C = 0{,}37$
Dimic /11/	$\beta = \left[1 - 5 \frac{1}{\sqrt{\pi}} (3 \cdot \zeta)^{-1/4} \cdot Ar^{1/4} \cdot Pr^{1/2} \cdot Ja \cdot Fo\right]^{1/5}$ $\beta = \left[1 - 7 \left(\frac{2{,}7}{\pi}\right)^{1/2} \cdot K_\sigma^{1/4} \cdot Ja \cdot Fo\right]^{1/7}$	for $Re > 3{,}1 \cdot K_\sigma^{0{,}25}$ with $\zeta = 2{,}61$ for $4{,}02 \cdot K_\sigma^{0{,}25} < Re < 3{,}1 \cdot K_\sigma^{0{,}25}$

Tab.1 : Some equations predicting the heat transport at condensing bubbles

The equations in this table can be summarized by the simple form

$$\beta = \frac{R}{R_0} = [1 - K\ Ja\ Fo] \tag{5}$$

where ß is the ratio of the momentary radius R of the bubble to its initial one, R_0, and where the factor K represents a constant or a function describing the heat transfer at the phase interface. Besides the Jacob-, Fourier-, and Prandtl-number also the Peclet-number

$$Pe = \frac{2\,R_0\,w_0}{a_F} \tag{6}$$

and the Archimedes-number

$$Ar = \frac{g\,(2\,R_0)^3}{\nu_F^2} \tag{7}$$

are used in some equations. Dimic /11/ introduced an additional dimensionless variable K

$$K_\sigma = \frac{R_0\,\sigma}{\rho_F\,a_F^2} \tag{8}$$

describing the influence of the surface tension. The agreement of data predicted with these equations is not too good which may be mainly due to the unknown heat transfer conditions. Nordmann and Mayinger /12/ therefore used the holographic interferometry to get a better inside into the thermo- and fluiddynamic behaviour at the phase interface and by this gaining information on the heat transport conditions.

2. Experimental Technique

To guarantee the boundary conditions as simple and homogeneous as possible the bubbles were produced by blowing saturated vapour into the subcooled liquid of the same substance in the experiments reported here. The nozzle for the injection of the steam is shown in Fig.1. The subcooled liquid was flowing slowly downward against the opening of the nozzle and of the bubble formed there. Special care was taken to guarantee saturation conditions on the vapour side of the phase interface by a special design of the nozzle. The nozzle consists of a short capillary having a diameter of 1,6 mm. The liquid in which the bubble is forming and in which it is collapsing was extremely carefully degased and then cooled down to a temperature temporally and locally as constant and homogeneous as possible. The latent heat of evaporation of the condensing vapour in the bubble is raising the temperature of the liquid. Therefore to guarantee that each bubble finds the same and equally subcooled temperature field the liquid flows with a velocity of approximately 2 cm/s downward against the nozzle. This small velocity does not influence the detachment and rising velocity of the bubble.

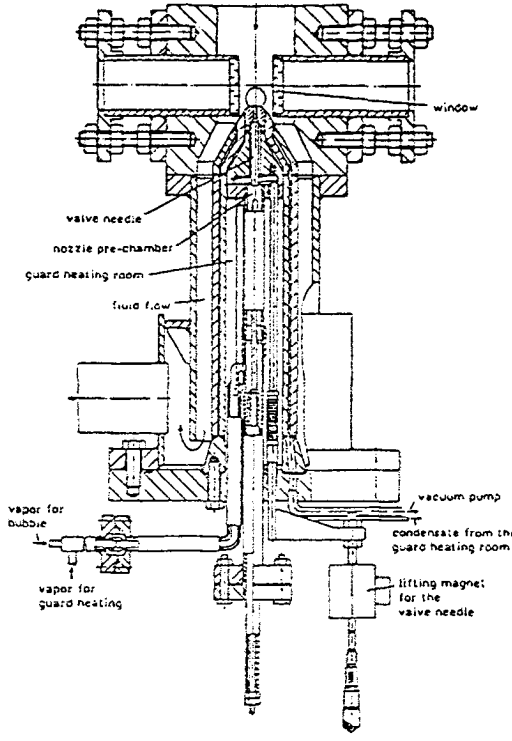

Fig.1 : Test section

The heat transfer at the phase interface was investigated by the holographic interferometry in connection with the high speed cinematography, as mentioned before. The arrangement of the used holographic set-up is schematically shown in Fig.2. Due to the small diameter of the bubble, the strong curvature of the phase interface together with the high temperature gradient in the boundary layer on the liquid side, the methods known in the literature - e.g. Abel-integral - are not sufficient to analyse and evaluate the interferograms. The deflection of the beam passing through the temperature field around the bubbles is not negligible, as assumed with the Abel-correction. Therefore, the theory for evaluating interferograms had to be extended. In detail the developed method for evaluating the interferograms is described in /13/.

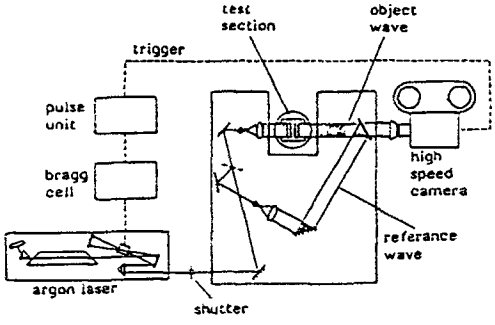

Fig.2 : Holographic interferometer

Knowing the temperature distribution around the bubble in the boundary layer of the liquid and derivating from this temperature distribution the temperature gradient, the heat transfer coefficient can be calculated with the well-known equation

$$h = \frac{-k\left(\frac{\partial T}{\partial y}\right)_w}{T_w - T_\infty} \qquad (9)$$

It can be assumed that the heat transfer resistance at the liquid side is large compared to that on the vapour side and, therefore, in pure substances - vapour and liquid consisting of the same substance - this heat transfer coefficient on the liquid side represents in its reciprocal value the total heat transport resistance with a good approximation.

With this holographic technique boundary layers down to 0,05 mm could be investigated with an accuracy good enough to predict the local heat transfer coefficient within 20%. In cases of still thinner boundary layers or with turbulent fluiddynamic conditions around the phase interface the heat transfer coefficient was evaluated from the temporal decrease of the bubble volume via an energy balance. This temporal decrease was measured with the high speed cinematography.

3. Experimental results

The scenarios of heat transfer controlled and inertia controlled condensation can be easily and well distinguished by measuring the pressure fluctuations around the bubble during condensation, especially at the end of the lifetime of the bubble. Fig.3 shows the maximum amplitudes of such pressure fluctuations as a function of the Jacob-number taken in water at system pressures between 0,25 and 4 bar. The amplitude in this figure is represented in a dimensionless form by reducing it with the system pressure and, by this, all measured data fall along a single line. This single line, however, shows a clear change in its gradient at a Jacob-number around 100. From this figure we can deduce that at Jacob-numbers higher than 100 inertia controlled condensation exists.

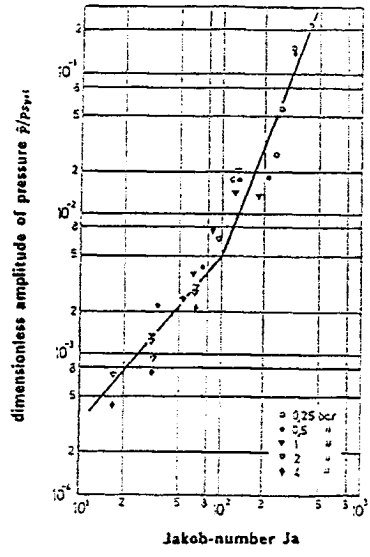

Fig.3 : Maximum pressure fluctuation at the end of decreasing volume as a function of the Jacob-number

The situation becomes much more complicated if we look in detail into the boundary layer around the condensing bubble. The temperature field in this boundary layer varies considerably not only with increasing Jacob-number but also for each single bubble during its lifetime, i.e. during its formation, detachment and condensation. These boundary conditions are also quite different at the bubble top and the bubble root, as Fig.4 demonstrates for the substance Propanol. The inter-

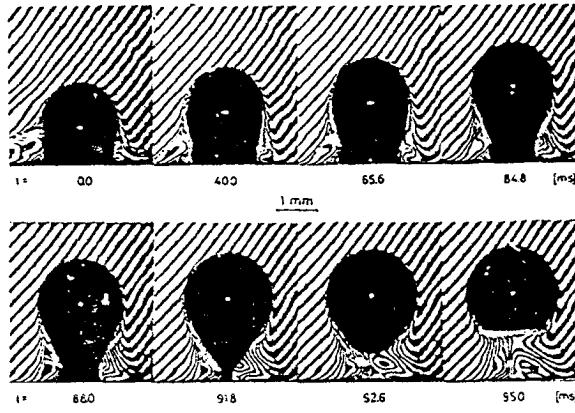

Fig.4 : Interferograms of a condensing propanol bubble (p = 2 bar, ΔT = 7.6 K, Ja = 7.1)

ferograms shown there were taken with the so-called finite fringe method and the deviation from the diagonal course of the fringes gives the temperature gradient and by this the heat transfer coefficient in a first approximation. Fig.5 presents the temporal course of the Nusselt-number at the top and the equator of a condensing steam bubble evaluated from interferograms /12/. Due to the growing of the bubble and the upward movement of its top the Nusselt-number increases at the beginning. When this period of growth is finished the Nusselt-number decreases again and reaches its minimum at the moment just before bubble detachment. After detachment there is a slight increase in the Nusselt-number due to the rising movement of the bubble.

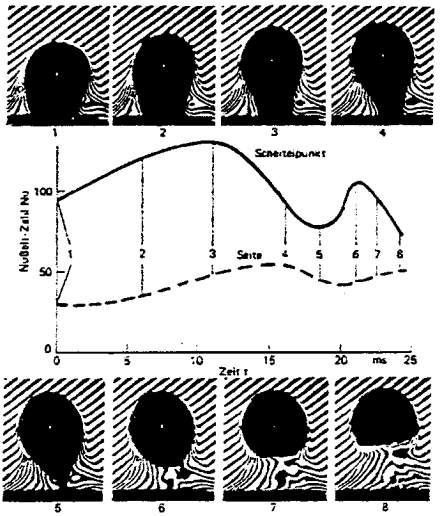

Fig.5 : Temporal course of Nu-number around a condensing bubble

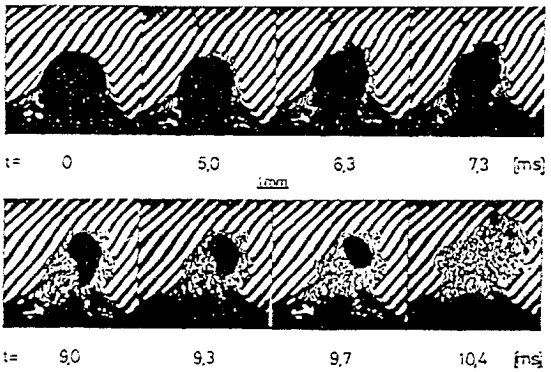

Fig.6 : Interferograms of a ethanol bubble with turbulent boundary layer
(p = 0.25 bar, ΔT = 20.6 K, Ja = 101.2)

With high Jacob-numbers which correspond to a much higher subcooling the situation around the bubble is completely different, as Fig.6 demonstrates. The phase interface becomes very early unstable due to local condensation effects and no laminar boundary layer can be observed around the bubble which condenses completely within approximately 10 m/s. Under these conditions the inertia of the liquid governs the bubble collapse. The influence of the Prandtl-number of the liquid onto the boundary layer demonstrates Fig.7 where interferograms of different substances for approximately equal values of Reynolds- and Jacob-numbers are compared. In this figure also data for the Nusselt-number and the heat transfer coefficient measured at the equator of the bubbles are shown. The Nusselt-number shows higher values with increasing Prandtl-number, however, regarding the heat transfer coefficient h the picture changes because the bubble diameter is used as characteristic length in the Nusselt-number and due to its higher surface tension water-bubbles grow to a larger diameter until detaching then the bubbles of hydro-carbon substances.

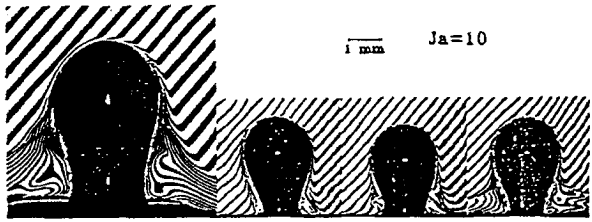

	Water	R113	Ethanol	Propanol
Re =	250	300	290	320
Pr =	1.97	5.7	9.0	14.4
Nu_{90} =	29	41	52	63
h =	5280 W/m^{2}K	1430	2930	3470

Fig.7 : Comparison of boundary layer conditions with various Prandtl-numbers

4. Empirical Correlations

The holographic interferograms showed at least at the top of the bubble an influence of the relative velocity between bubble and liquid onto the heat transfer coefficient and by this onto the Nusselt-number respectively, similar to that of a solid sphere under cross flow conditions. Therefore it was obvious to make a first trial for correlating the heat transfer by using the well-known equation

$$Nu = 2 + C\, Re^{m}\, Pr^{n} \qquad (10)$$

which is valid for Reynolds-numbers between 0 and 200. In our experiments the Reynolds-numbers were always above 100 and reached up to 1000. Therefore pure conduction expressed by the 2 in Equ.(10) was of neglectible influence on the results and Equ.(10) was simplified into the form

$$Nu = C\, Re^{m}\, Pr^{n} \qquad (11)$$

Using the bubble diameter at the moment of detachment as characteristic length in the Nusselt- and Reynolds-number and by carefully averaging the measured results the correlation

$$Nu = 0.6\, Re^{0.6}\, Pr^{0.5} \qquad (12)$$

was found for describing the mean heat transfer coefficient during the period when the bubble is still connected with the nozzle, i.e. before the bubble detachment. This equation is experimentally verified for Reynolds-numbers between 100 and 1000, Prandtl-numbers between 6 and 20 and Jacob-numbers between 5 and 40. The equation is based on the assumption that the heat transport resistance is only on the liquid side which is certainly true for pure vapour, not containing non-condensable gases. A comparison between experimental data measured by the holographic interferometry and the predictions of Equ.(13) is shown in Fig.8. The heat transfer at the surface of a bubble sticking at a nozzle but exposed to a slow cross flow is higher than that around a solid sphere due to the smaller shear stress at the phase interface and due to the movability of the bubble surface.

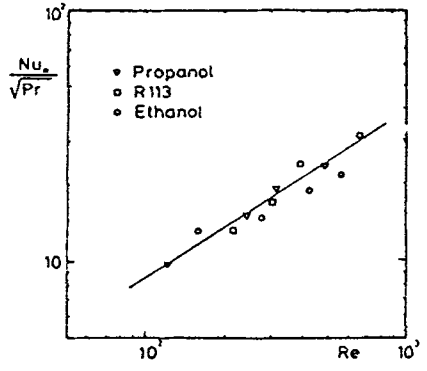

Fig.8 : Comparison of experimental data (holographic interferometry) with empirical correlation

With rising bubbles, i.e. after detachment, the heat transfer conditions become more complicated. Due to condensation the bubble diameter decreases continuously while the bubble is rising. Using the instantaneous bubble diamter would need a rather extensive and iterative procedure for calculating the heat transfer. In the literature, however, reliable equations can be found for correlating the bubble diameter in the moment of bubble detachment. Therefore, and with respect to a simpler procedure for practical use, the bubble diameter at the moment of detachment was used for correlating the heat transfer. The bubble diameter at this moment can be easily predicted by Equ.(13)

$$d = \sqrt[3]{\frac{6\,\sigma\,d_{Dü}}{\Delta\varrho\,g}} \qquad (13)$$

Using this diameter the experimental results could be correlated in the simple form

$$Nu = 0.185\ Re^{0.7}\ Pr^{0.5} \qquad (14)$$

representing now data up to Reynolds-numbers of 10^4. The low value of 0,185 of the constant in Equ.(14) is because of using the detachment diameter as characteristic length.

As shown in Fig.9 this correlation corresponds well with measured data for different substances and from different origin in the literature. The correlation can be used up to a Jacob-number of approximately 80, as long as inertia effects do not play a dominant role.

The highspeed cinematography gives the best information about the temporal decrease of the bubble diamter which, of course, is closely related with the heat transfer at the phase interface. The duration of the bubble life can be expressed by the Fourier-number in a dimensionless form and by using the simple correlation

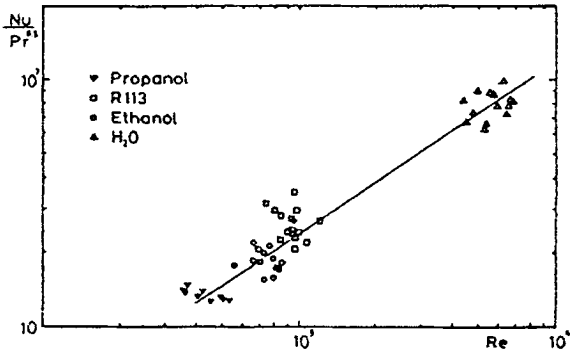

Fig.9 : Mean Nusselt numbers of rising bubbels, comparison with equation 14

$$Fo = 1.784\ Re^{-0.7}\ Pr^{-0.5}\ Ja^{1.0} \qquad (15)$$

Up to a Jacob-number of 60 this equation corresponds well with the measured data, as Fig.10 shows. For higher Jacob-numbers the measured data deviate due to the fact that now inertia effects have increasing influence slowing down the speed of condensation. Equ.(15) was derived from the heat transfer correlation (14).
The temporal decrease of the bubble diameter can be predicted by using Equ.(16)

$$\beta = \left[\ 1 - 0.56\ Re^{0.7}\ Pr^{0.5}\ Ja\ Fo\right]^{0.9} \qquad (16)$$

which was correlated from the data measured in /12,13/.

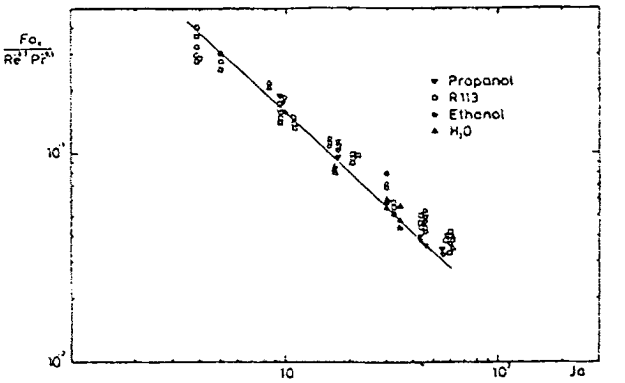

Fig.10: Condensation time,comparison of measured data and equation 18.

5. Conclusions

The measurements with the holographic interferometry and the high speed cinematography showed that heat transfer and volumetric decrease of pure vapour bubbles condensing in a subcooled liquid of the same substance can be reliably correlated by using three dimensionless numbers, namely the Jacob-, the Reynolds-, and the Prandtl-number, as long as the condensation velocity is controlled by heat transfer effects. The Jacob-number gives a clear indication whether the heat transfer or the inertia is dominant in the condensing process. Up to Jacob-numbers of 60 - 80 the condensation is purely controlled by the heat transfer at the phase interface. After a transition situation - heat transfer and inertia - with Jacob-numbers higher than 100 inertia starts to become the exclusive effect. For calculating the condensation rate at this situation the Rayleigh correlation /5/ can be used as Plesset /3/ and Hammit /4/ showed.

REFERENCES

/1/ Hammit, F.G.
Cavitation and multiphase flow phenomena.
McGraw-Hill Inc. (1980).

/2/ Theofanous, T.G.; Biasi, L.; Isbin, H.S.; Fauske, H.K.
Non-equilibrium bubble collapse - a theoretical study.
Chem.Eng.Prog.Symp.Ser., Vol.66, 102, S.37-47 (1970).

/3/ Plesset, M.S.
J. Appl. Mech. 16, S.277-282 (1949).

/4/ Hammit, F.G.; Kling, C.L.
A photographic study of spark-induced cavitation bubble collapse.
J. Basic Eng. 94, S.825-833 (1972).

/5/ Rayleigh, L.
On the pressure developed in a liquid during the collapse of a spherical cavity.
Phil. Mag. 34, S.94-98 (1917).

/6/ Moalem, D.; Sideman, S.
The effect of motion on bubble collapse.
Int. J. Heat Transfer 16, S.2321-2329 (1973).

/7/ Akiyama, M.
Bubble collapse in subcooled boiling.
Bulletin of the JSME 16, 93, S.530-575 (1973).

/8/ Voloshko, A.A.; Vurgaft, A.V.; Aksel'rod, L.S.
Condensation of vapour bubbles in a liquid.
Translated from Theoreticheski Osnavy
Khimicheskai, Tekhnologii, Vol.7, No.2, S.269-272 (1973).

/9/ Florschuetz, L.W.; Chao, B.T.
On the mechanics of vapour bubble collapse.
J. Heat Transfer 87, S.209-220 (1965).

/10/ Voloshko, A.A.; Vurgaft, A.V.
Study of condensation of single vapour bubbles in a layer of subcooled liquid.
Heat-Transfer-Soviet Research, Vol.3, No.2 (1971).

/11/ Dimic, M.
Collapse of one-component vapour bubbles with translatory motion.
Int. J. Heat Mass Transfer 20, S.1322-1325 (1977).

/12/ Nordmann, D.; Mayinger, F.
Temperatur, Druck und Wärmetransport in der Umgebung kondensierender Blasen.
VDI Forschungsheft Nr.605, S.3/36 (1981).

/13/ Chen, Y.M.
Wärmeübergang an der Phasengrenze kondensierender
Blasen.
Diss. Techn. Universität München (1986).